Karlsruhe Institute of Technology

Modelling of Massive Gas Injection with Tokamak Code TOKES for ITER Disruption Mitigation Design

I.S. Landman[1], S.E. Pestchanyi[1], Y. Igitkhanov[1], R. Pitts[2]

[1]Karlsruhe Institute of Technology, IHM, P.O. Box 3640, 76021 Karlsruhe, Germany

[2]ITER International Team, Cadarache, France

Introduction: In tokamaks the damage to PFCs after the disruptions can be mitigated using preventive massive gas injection (MGI) of noble gases into confined plasma during the thermal quench (TQ). The gas gets ionized and the plasma contamination results in fast loss of plasma energy by radiation distributed over the wall. The injection of noble gases into deuterium confined plasma was tested on the tokamaks e.g. JET and DIII-D. Experiments demonstrated effective ionizations of G-atoms (G = Ne, Ar, He) at the plasma edge, and following MHD unstable modes which cause a thermal quench (TQ) by radiating plasma energy. The MHD activity and enhanced mixing of G-ions were mainly detected when the ionization cooling front reached the magnetic surface of safety factor q = 2.

The ITER MGI issues such as distribution of radiation power over the vessel wall can be addressed numerically. For the modelling the integrated tokamak code TOKES is applied [1,2]. Detailed two-dimensional radiation fluxes and the expansion of noble ions both across and along the magnetic surfaces are simulated. In the work MGI model of TOKES is applied for the whole tokamak vessel for argon MGI into ITER deuterium confined plasma with assessments of strongly varying radiation fluxes from the contaminated plasma onto beryllium wall and following maximal wall temperature.

Main features of integrated tokamak code TOKES [3]

- The Grad-Shafranov equation is solved at each time step. Plasma shape is provided calculating the currents in the poloidal field coils.
- The confined multi-fluid plasma transport is based on the gyro-Bohm model with account for neo-classical effect and the Troyon's β-limit.
- For modelling of neutral atoms, photons and neutrons the Monte-Carlo method is applied. Random rays of neutrals propagate through triangle-shaped meshes.
- The processes of heat transport in the wall, sputtering, surface evaporation, and ionization of propagating atoms are implemented.
- Ions are described in terms of level population densities N_{mzk}, with the indices m for species from H to W, z charge state and k electron energy levels.
- Radiation transport contains bremsstrahlung, recombination and line emission.

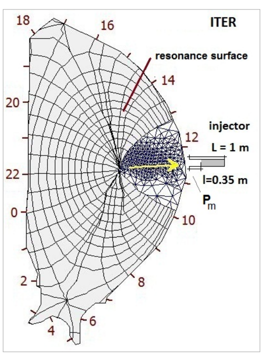

Fig. 1 Layout of ITER as simulated. Magnetic flux coordinates (x,y), the coordinate X along wall surface, and minor radius axis a. A fragment of underground triangular meshes is shown as well.

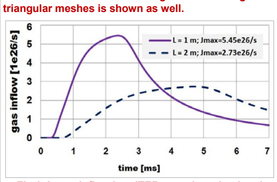

Fig 2 Argon inflow into ITER vessel as simulated

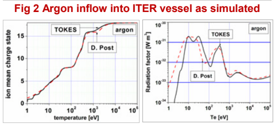

Fig. 3 Validations of radiation model by Ref.[4]

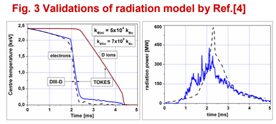

Fig. 4 Validation of TOKES by DIII-D centre electron temperature and radiation power.
(k_{ec} electron classical thermal conductivity.)

Implications of ITER MGI modelling: The purpose is minimization of wall temperature T_w at most heated location P_m (see Fig. 1) keeping short cooling time τ_{cool}. Plasma thermal energy $E_0 \approx 420$ MJ. The injector is placed at P_m. Injector length L = 1 or 2 m. G-gas initial temperature 310 deg(K). Maximal inflow J_{Gmax} determines MGI process. Time t = 0 is the moment of opening injector's valve situated at $l = 0.35L$. Initial wall temperature 500 K, beryllium thermal conductivity k_w = 70 W/K/m, thermal capacity C_w = 5.7 MJ/K/m³. With τ_{cool} ~ 5 us thin skin layer is heated, its thickness $\Delta_{wsub} \sim (\tau_{cool} k_w / C_w)^{1/2} \approx 0.25$ mm.

The G-ions fast occupy periphery area and the process transforms into cross-propagating cooling wave (see Figs. 5,6). Behind the cooling front runaway electrons may appear. Here we don't address them (admitting their importance after TQ). However, in our model they are implied in order to keep plasma currents and magnetic field B fixed. Thus they prevent deposition of magnetic energy at the cooling front and in electric skin layer of the wall during MGI thermal quench.

The validation by Ref.[2] (Fig. 4) provided $k_{e\perp} = f_e k_{e\perp cl}$ with $f_e = 7\times10^5$, i.e. $\chi_{e\perp} = 2k_{e\perp}/3n_e \approx 140$ m²/s (B = 2.1 T, $n_e = 8\times10^{19}$ m^{-3}, and T_e = 2.5 keV in DIII-D core) which significantly exceeds ~1 m²/s expected at normal operation: MGI triggers some anomalous transport. For ITER some other $\chi_{e\perp}$ and f_e must be used.

We suggest a scaling for $\chi_{e\perp}$ assuming that thermal cross-transport increases due to small deteriorations of toroidal symmetry and thus slight overlapping of nested magnetic surfaces ('3D transport'). In 3D transport classical longitudinal conductivity $k_{e||cl} = 3.2 n_e T_e \tau_e / m_e$ is involved. We assume also pressure change $\Delta p = p(t,x,y) - p_0(x)$ to cause symmetry breaking of field B, thus without it global 3D transport cannot start. The radiating wave is taken into account by using the ratio $\eta = E_{rad}/E_0$, because radiated energy $E_{rad} \approx (3/2)\int(p_0 - p)dV$.

Making scaling to ITER, $k_{e||cl}$ is multiplied by a factor $f_{e||}$ and equated to the validated $k_{e\perp}$: $f_{e||} = f_{e||a} = (f_{ea} k_{e\perp cl}/k_{e||cl})_{DIII-D} \approx 2.6\times10^{-9}$. This value of $f_{e||}$ is also used for ITER: $k_{e\perp} = k_{e\perp cl} + \eta f_{e||} k_{e||cl}$. For $n = 1.7\times10^{20}$ m⁻³ and T = 15 keV in ITER core $\chi_{e\perp ITER} \approx 5\times10^3 \eta$ m²/s follows.

Plasma: 2D multi-species plasma is implemented in the whole vessel of arbitrary shape obeying the toroidal symmetry. The code calculates non-stationary radiation losses (without reabsorption) coupled with populations of different charge states (Fig.3), and gas motion in the injector tube (Fig.2). Some algorithms (e.g. for normal operation regime) are not used in order to focus on MGI thermal quench during ~3-7 ms.

Magnetic flux coordinate (MFC): The models use poloidal magnetic flux $w(r,z)$ (Fig.1) and the cylindrical coordinates (r,z). The magnetized plasma is numerically organized as many toroidal finite elements ('cells') along the contours of constant w. The magnetic surfaces built from x–points subdivide the vessel's poloidal plane area into a number of 'maps'. The maps are most thick layers possible. The flux w across a map varies monotonically between its borders.
Then the curves that go along ∇w are built from each x-point. Such a curve can cross several maps. Those paths ('cuts') subdivide each map into several 'domains'. The domains offer largest possible cells. To get small cells, the domains are subdivided inserting additional cells. The cells are prescribed sizes h_x and h_y along x- and y-coordinates.

Conclusions: TOKES simulations for ITER's argon injection demonstrated that at maximum inflow $J_{Gmax} < 2\times10^{26}$/s maximum beryllium wall temperature T_{wmax} gets below melting point T_{melt}. TQ time τ_{cool} weakly increases with injector length L. Increasing J_{Gmax} from 10^{26}/s by 5 times results in dropping τ_{cool} from 6 ms by 2 times. To avoid Be melting τ_{cool} > 4 ms is needed. Several powerful flushes accompany plasma cooling, which makes T_{wmax} a stochastic value scattered for ~100 deg.

For beryllium wall, melt free MGI is hardly predictable because T_{wmax} is obtained for the needed narrow range of τ_{cool} (3 to 6 ms) in vicinity of T_{melt}. Furthermore, magnetic energy release at cooling front (with following transformation into radiation) and in the wall may increase T_{wmax}. Therefore some other material is desirable at most loaded position.

Validation of suggested scaling for thermal transport is needed. T_{wmax} varies depending on injector position, injected gases and appearance of runawas during TQ, which is going to be investigated in course of next validations.

Validation of TOKES by DIII-D experiment:
Fig. 4 (left) demonstrates the comparison of simulated and experimental centre temperature $T_{e0}(t)$. The fitting is achieved tuning up a few parameters which are not precisely known in the experiment but strongly influence $T_{e0}(t)$. Main of them is electron thermal conductivity $k_{e\perp}$ of hot plasma (before and after cooling wave reached resonance surface).

The good fitting indicates that the simulation reproduces main processes of TQ. First consequence of core instabilities appears to be small deteriorations of toroidal symmetry and thus slight overlapping of nested magnetic surfaces, which drastically increases electron cross-transport by thermal conductivity along entangled magnetic field lines ('3D transport'). At start of cooling the periphery the instabilities can develop at many rational values of q in the core. We assume they remain moderate until $t > t_{q2}$.

Fig. 4 (right) compares radiation power $P_{rad}(t)$. The code calculates the plasma radiation rather realistic. The simulation cannot properly describe the initial stage (t < 1.5 ms). We attribute the difference to the fact that real 3D jet penetrates much smaller part of plasma periphery than the numerical jet does. Initially real expanding contamination does not yet occupy outer magnetic surfaces therefore the radiative cooling surface is still small, which decreases P_{rad} at t < 1.5 ms and increases it at later time.

Results of ITER MGI simulations: To clarify cooling time, calculations for L = 1 and 2 m are performed varying J_{Gmax}, with 41 plasma layers inside the separatrix and triangle sizes ~3 cm in front of injector.

Figs.5,6 demonstrates propagation of cooling wave. After reaching resonance surface at t = 3.4 ms cooling wave remarkably increases speed, which can be due to hot recombined G-ions coming from behind the front with large velocities ~2 km/s. Profile of T_e gets steep near the front, which is typical when $k_{e\perp}$ strongly increases with T_e ($k_{e\perp} \propto T_e^{5/2}$).

Fig.7 shows calculated cooling times. For the moment of E_{rad}/E_0 = 0.83 (83% cooling) τ_{cool} drops from 4.8 ms (L=1 m) and 5.7 ms (L=2 m) at $J_{Gmax} = 10^{26}$/s down to 2.3 ms (L=1 m) and 3.7 ms (L = 2 m) at $J_{Gmax} = 5.5\times10^{26}$/s. It is to note rather non-monotonic (stochastic) local behaviour of τ_{cool}.

Fig.8 shows maximal wall temperatures, it happens always at X = 11.5 m (P_m, injector location). Stochastic behaviour of T_{wmax} is seen as well. Wall surface melts at $J_{Gmax} > 2\times10^{26}$/s (in some 'average sense').

Fig.9 helps for explanation of stochastic behaviour. The calculated transformation of plasma energy into radiation on the cooling front is very non-regular and consists of several powerful flushes up to 1 TW. During those pulses T_w substantially increases at wall surface, and in pauses T_w slowly decreases due to heat withdrawal into wall bulk. T_w reaches maximum after last flush. If last flush occurred at the end of cooling (see Fig. 9) T_w gets larger by 100-200 deg and can most probably overcome melt threshold.

Figs.10,11 demonstrate distribution of radiated power and following wall surface temperature over the entire vessel surface.

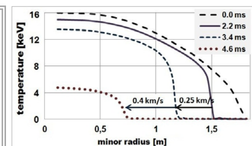

Fig. 5 Electron temperature (L = 2 m, $J_{Gmax} = 2\times10^{26}$/s)

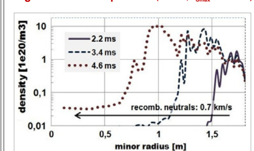

Fig. 6 Calculation of argon density

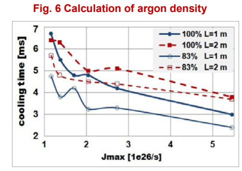

Fig. 7 Argon MGI cooling time: 100%: $E_{rad} = E_0$

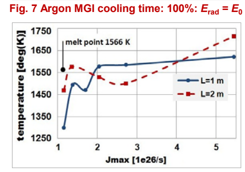

Fig. 8 Maximal wall temperature T_{wmax} (at P_m)

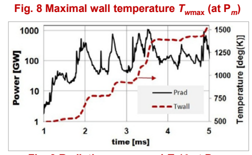

Fig. 9 Radiation power and $T_w(t)$ at P_m (L = 2 m, $J_{Gmax} = 2\times10^{26}$/s)

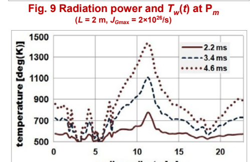

Fig. 10 Wall surface temperature vs. X (L = 2 m, $J_{Gmax} = 2\times10^{26}$/s)

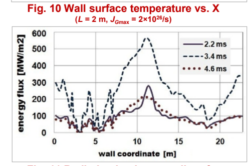

Fig. 11 Radiation load onto wall surface (L = 2 m, $J_{Gmax} = 2\times10^{26}$/s)

Acknowledgement: This work, supported by the European Communities under the EFDA Task Agreement WP11-PWI between EURATOM and Karlsruhe Institute of Technology, was carried out within the framework of the European Fusion Development Agreement. The views and opinions expressed herein do not necessarily reflect those of the European Commission.

Refs.: [1] I.S. Landman et al 2010 Fusion Eng. Des. doi:10.1016/j.fusengdes.2010.12. 017
[2] I.S. Landman et al 2010 Fusion Eng. Des. 85 1366
[3] E.M. Hollmann et al., Nucl. Fus. 48 (2008) 1
[4] D.E. Post et al., Atomic Data and Nuclear Data Tables, 20 (1977) 397

E-mail: igor.landman@kit.edu

The Institute for Pulsed Energy and Microwave Technology